Chapter 3

OPTICALLY DETECTED MAGNETIC RESONANCE OF DEFECTS IN 4H-SIC

3.1 Principles of ODMR

Optically detected magnetic resonance (ODMR) refers to optical readout of qubit spin states or optical polarization of spin states using microwave fields driving the resonance between different spin states. This effect is very useful in developing different optical quantum technologies. The signal of ODMR is the optical signal emitted by the optically addressable qubits in the ZPL or the phonon sidebands. Depending on the population ratio between different spin sublevels, the ZPL counts either increase or decrease. This contrast of ZPL counts gives information about spin polarization. For PL1 and 2 c-axis aligned divacancies in 4H-SiC, this is enabled by the non radiative decay path, so called intersystem crossing between the excited and ground triplet states [41, 44], with level structures similar to negatively charged nitrogen vacancy centers in diamond[43, 47, 69]. Microwaves are used to resonantly address different spin sublevels, which generates different optical emission intensity. A simplified energy level structure and ODMR mechanism for c-axis divacancies is shown in figure 3.1.

In the left side of the figure3.1, microwaves are off and divacancies are continuously excited non resonantly. Excited divacancies emit photoluminescence through spin conserving relaxation. The excited $m_s = \pm 1$ sublevels in excited states are more strongly coupled to singlet states that lie between the triplet states, which gives rise to non radiative relaxation. These singlet states are believed to be preferentially coupled to the ground $m_s = 0$ sublevel. Therefore continuous optical cycling between excited and ground triplet states will result in most divacancies populated in $m_s = 0$ sublevel. Because divacancies in excited $m_s = \pm 1$ sublevels have higher possibility to go through non radiative relaxation, there are less photon counts if more divacancies are populated in ground $m_s = 0$ sublevel. In the beginning of optical excitation/initialization, ZPL is darker as there are almost equal population in $m_s = 0$ and $m_s = \pm 1$ sublevel. However, continuous optical excitation will eventually achieve non- Boltzmann steady state with most spins to $m_s = 0$ and reach brighter ZPL emission.

In the right side of the figure, a microwave field is used to drive the spin transition. When the microwaves are on and the frequency is resonant with the energy gap between ground $m_s = 0$ and $m_s = \pm 1$ sublevels, the microwaves pump some of the population in the $m_s = \pm 1$ state, which leads to a change in the emitted photoluminescence. When the microwaves are not resonant with the spin transition there is no significant effect on the luminescence.

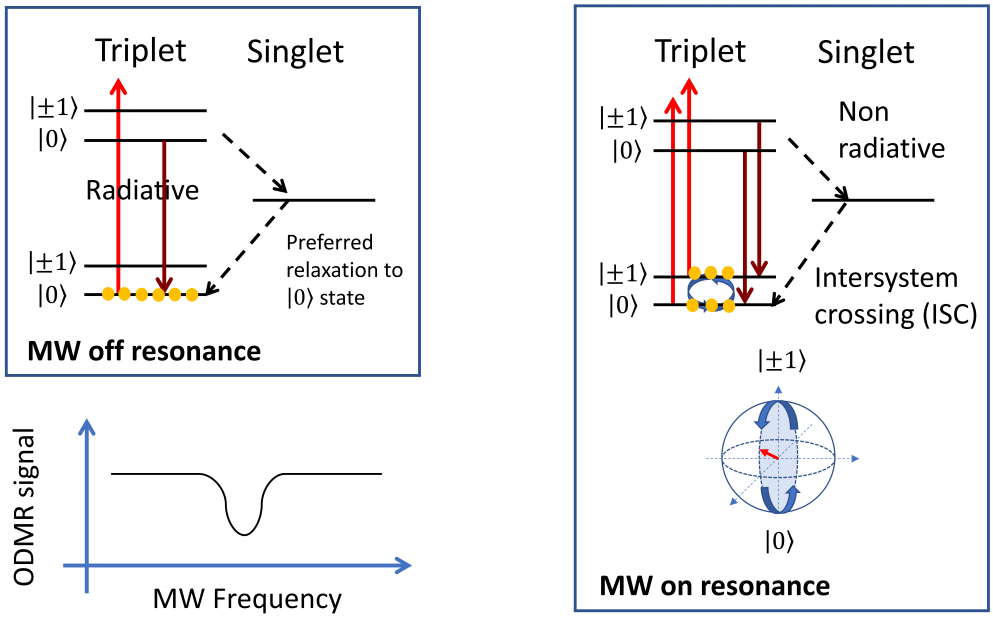

Figure 3.1: Spin population and ODMR signal change when microwave is on/off

3.2 ODMR setup

Our final ODMR setup uses a microwave (MW) line deposited on the SiC samples directly as shown in figure 3.2. The design was inspired from Koehl et al. [32] supplementary material. We glued a round PCB board around the copper cold finger and the gold MW lines (the design is shown in figure 3.2) were wire bonded to conductive segments on the board. Those segments were connected to an external SMA port with soldered wires (figure 3.3). The first version with a single wire put across the samples didn't provide good attachment to samples and the wire was prone to separation from the sample surface. With higher power MW applied in cryostat, the wire often moved away or across samples due to heat expansion resulting in weak MW drive amplitude on sample surface.

The ODMR signal shown in our results was defined by the equation shown in figure

3.4. ZPL of each divacancies was spectrally filtered by adjustable long pass and short pass filters. ODMR is the contrast of filtered ZPL with MW applied and ZPL without MW applied. As you can see in the typical spectrum of Cr implanted 4H-SiC or undoped 4H-SiC, PL4 is bright and its phonon side band counts of PL4 is comparable to ZPL of PL3, also lying on PL1 and PL2. This creates overlap of PL4 ODMR signal on PL1-3 ODMR signal that will be shown in the next section.

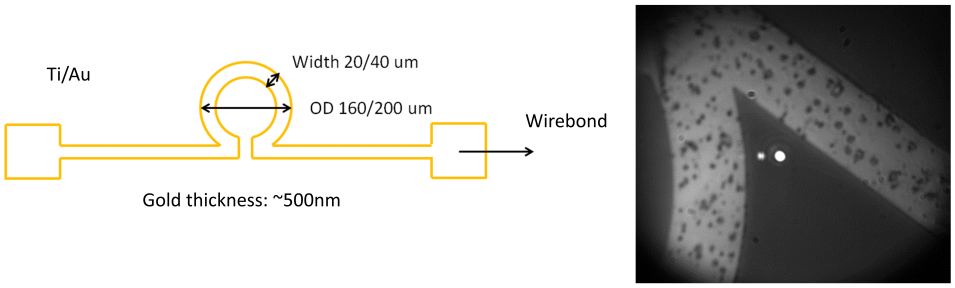

Figure 3.2: Schematic of the MW gold line deposited on a 4H-SiC sample. The right figure shows the image taken from CCD camera with 780nm excitation laser on.

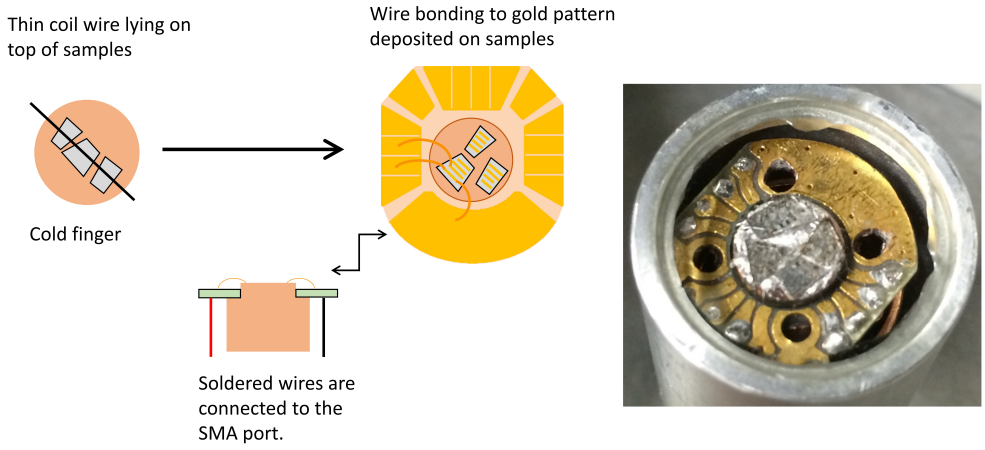

Figure 3.3: MW setup around samples. Initial setup with a single wire on samples is replaced with more robust method with wire bonding and gold line deposition directly on sample.

3.3 ODMR results on ensemble divacancies and on Cr ions

We observed similar ODMR signal to that shown in literature of divacancy ODMR [32]. The measurements were performed on highly purified semi insulating (HPSI)

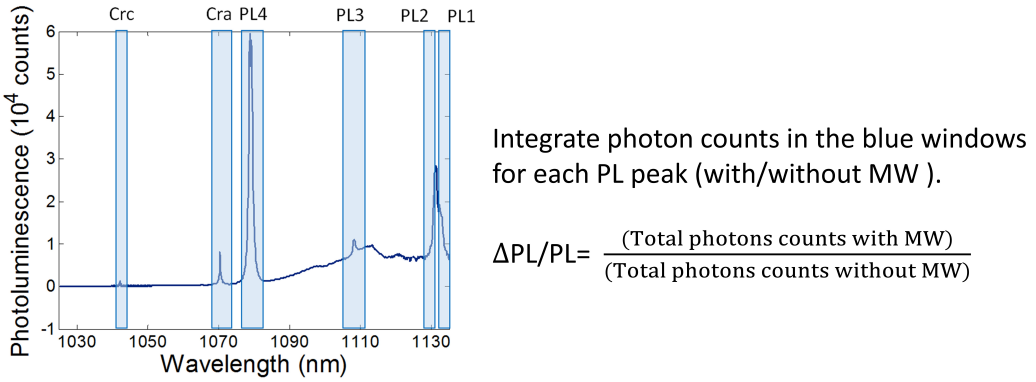

Figure 3.4: ODMR signal collection method

4H-SiC sample from CREE Inc without any post processing. Divacancies observed in this sample are incorporated intrinsically. Most of divacancies ODMR signal is in the range of 1.28-1.38 GHz. The comparison of our results (left) and the results from [32] (right) is shown in figure 3.5. Our ODMR signal peaks are generally broader than theirs, which suggests a power broadening effect considering that they used the same type of HPSI 4H-SiC samples. ODMR signal of PL3 at approximately 1.305 GHz is overlapped with background PSB ODMR signal of PL4. However PSB of PL4 on PL1 and PL2 ZPL is much smaller than their ZPL and there's no noticeable PL4 influence. Figure 3.6 shows a wide range of ODMR signals. A signal at 1.45 GHz is an artifact due to heating of the sample and change of the focus. You can see larger power broadening with larger MW power as shown in figure 3.7. The power label at the left side is the MW source power and this is amplified by 20dB through amplifier before MW is delivered to the sample gold lines.

ODMR measurements on Cr ions on Cr implanted 4H-SiC was attempted both with and without magnetic field. As zero field splitting parameter D of Cr_A and Cr_C was known to be <1.2 GHz and ~ 6.0 GHz by Son et al. [48], we applied magnetic field to c-axis direction for 0.15 T, which gives expected ODMR signal around 1.7 GHz. We observed PL1 and PL2 ODMR at corresponding magnetic field calculated with $2g\mu_B B/h$ at around 2.75 and 2.78 GHz as shown in figure 3.8 but we didn't observe any ODMR signal from Cr_C with this continuous wave ODMR method.

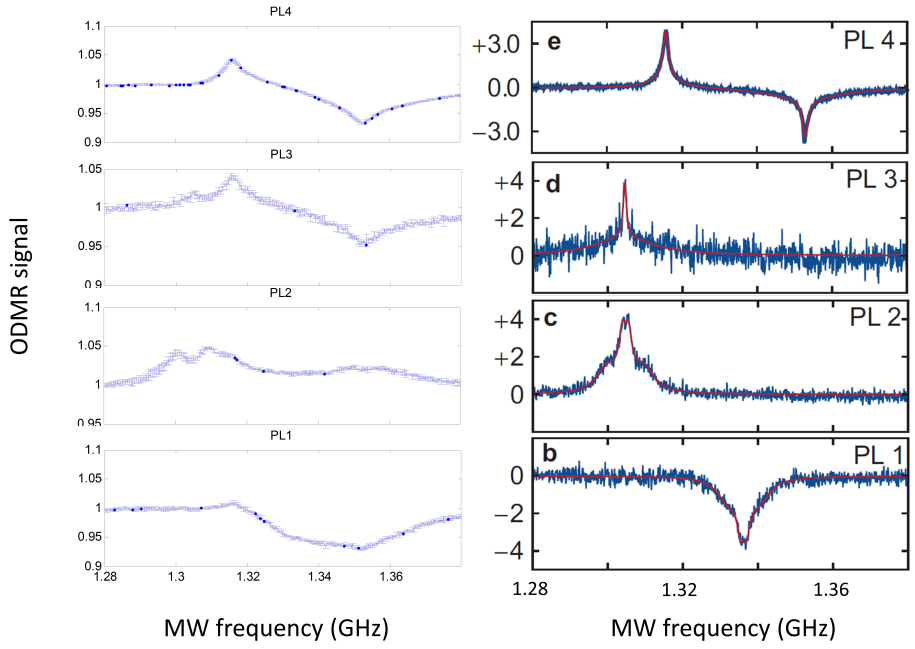

Figure 3.5: Our ODMR signal collected on undoped HPSI 4H-SiC at liquid helium temperature (~20 K) at left side. Right side shows results from Koehl et al. [32]

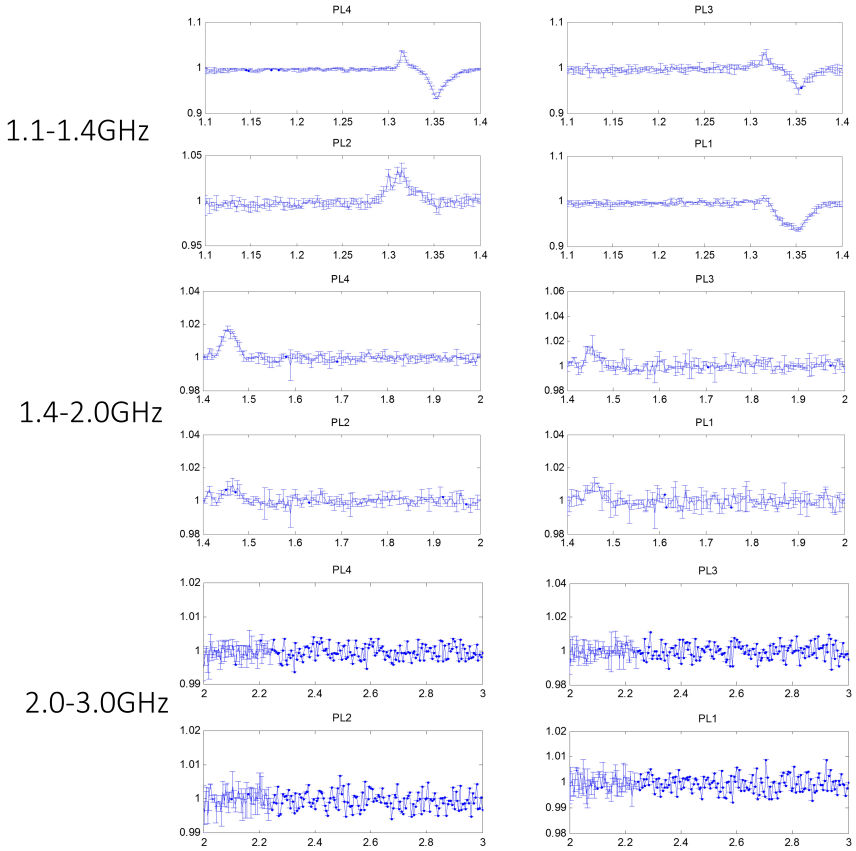

Figure 3.6: ODMR signal collected on undoped HPSI 4H-SiC at liquid helium temperature (~20 K) with wider MW sweep range.

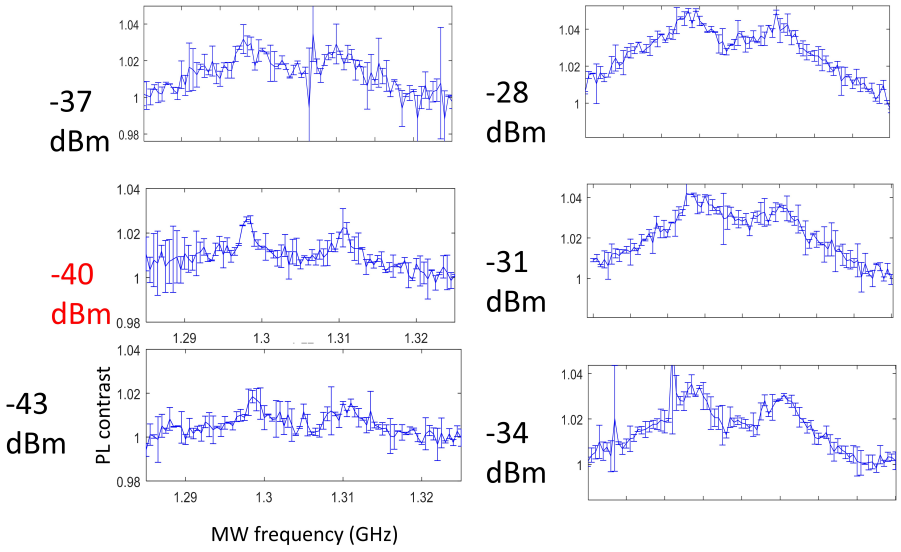

Figure 3.7: Power broadening of ODMR signal of ensemble divacancies PL2

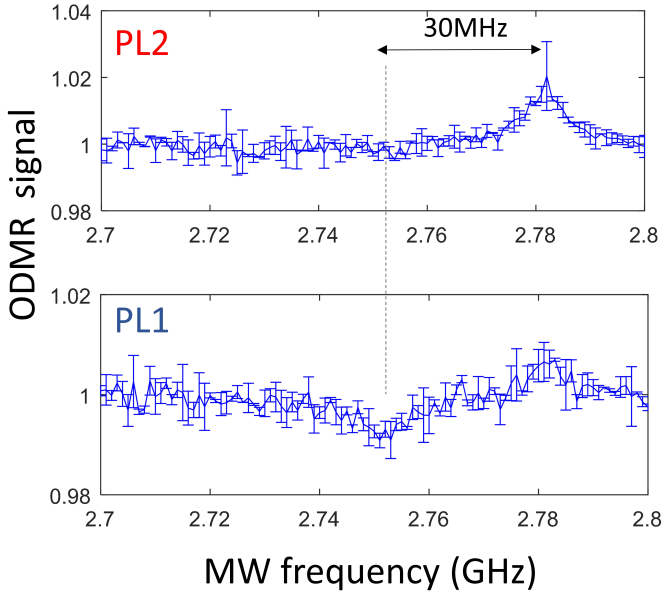

Figure 3.8: ODMR signal of PL1 and PL2 divacancies in Cr implanted 4H-SiC under 0.15 T at liquid nitrogen temperature.